Research Square

Preprints are preliminary reports that have not undergone peer review.
They should not be considered conclusive, used to inform clinical practice,
or referenced by the media as validated information.

Histopathological alterations of deep cervical lymph nodes in Alzheimer's disease and their association with cognitive decline

Gechang Cheng
Xiangya Hospital Central South University
Huahui Hu
Xiangya Hospital Central South University
Jian Mao
Xiangya Hospital Central South University
Yafang Zhou
Xiangya Hospital Central South University
Liming Qing
Xiangya Hospital Central South University
Panfeng Wu
Xiangya Hospital Central South University
Juyu Tang
tang.juyu@csu.edu.cn

Xiangya Hospital Central South University

Article

Keywords: Alzheimer’s disease, deep cervical lymph nodes, germinal centers, meningeal lymphatic drainage, postoperative prognosis

Posted Date: November 3rd, 2026

DOI: https://doi.org/10.21203/rs.3.rs-10450478/v1

License: This work is licensed under a Creative Commons Attribution 4.0 International License.
Read Full License

Additional Declarations: No competing interests reported.

Histopathological alterations of deep cervical lymph nodes in Alzheimer's disease and their association with cognitive decline

Gechang Cheng[1#] Huahui Hu[1#] Jian Mao[2] Yafang Zhou[2] Liming Qing[1] Panfeng Wu[1] Juyu Tang[1,3]

[1]Department of Orthopedics, Hand and Microsurgery, Xiangya Hospital, Central South University, Changsha, Hunan, 410008, China

[2]Department of Neurology, Xiangya Hospital, Central South University, Changsha, Hunan, 410008, China

[3]National Clinical Research Center for Geriatric Disorders, Xiangya Hospital of Central South University, Changsha, Hunan, 410008, China.

# These authors contributed equally to this work as the co-first authors.

Correspondence: Juyu Tang(tangjuyu@csu.edu.cn) | Panfeng Wu (wupanfeng@csu.edu.cn) | Liming Qing (qingliming0338@163.com)

Keywords: Alzheimer’s disease; deep cervical lymph nodes; germinal centers; meningeal lymphatic drainage; postoperative prognosis

Abstract

Background

Alzheimer’s disease (AD) is characterized by progressive cognitive and functional decline with amyloid-beta (Aβ) and tau pathology. In addition to abnormal protein aggregation, impaired clearance of brain-derived solutes through glymphatic and meningeal lymphatic pathways may contribute to disease progression. Deep cervical lymph nodes (DCLNs), as major downstream lymphoid structures of central nervous system drainage, may provide a peripheral histological window into the brain-cervical lymphatic axis. However, whether human DCLNs undergo histopathological remodeling in AD and whether such changes are clinically relevant remain unclear.

Methods

DCLNs were obtained from 66 participants, including 59 patients with moderate-to-severe AD and 7 cognitively unimpaired controls. Hematoxylin and eosin staining was used to assess lymph node morphology and germinal center (GC) abundance. Multiplex immunofluorescence was performed to evaluate Aβ, tau, alpha-smooth muscle actin (alpha-SMA), CD31, and LYVE-1. Cognitive and functional status were assessed using the Mini-Mental State Examination (MMSE), Clinical

Dementia Rating-Sum of Boxes (CDR-SB), and Activities of Daily Living (ADL) scores. AD patients were stratified by GC abundance using a cutoff of 4 GCs. Multivariate logistic regression, receiver operating characteristic analysis, decision curve analysis, and 6-month postoperative follow-up were performed.

Results

DCLNs from patients with AD showed histopathological remodeling, including reduced GC abundance, structural disruption, fibrosis-related stromal changes, altered vascular and lymphatic marker expression, and detectable Aβ and tau immunoreactivity. Compared with patients with >4 GCs, those with ⩽4 GCs had worse baseline cognitive and functional status, including lower MMSE scores and higher CDR-SB and ADL scores. In multivariate analysis, higher alpha-SMA mean fluorescence intensity was associated with a lower likelihood of preserved GC abundance, whereas higher MMSE score was associated with preserved GC abundance. Patients with >4 GCs also showed greater improvement in MMSE, CDR-SB, and ADL scores at 6 months postoperatively.

Conclusions

Human DCLNs exhibit histopathological remodeling in AD. Reduced GC abundance is associated with greater clinical impairment, fibrosis-related remodeling, and poorer 6-month postoperative improvement, suggesting that DCLN histopathology may have potential clinical and prognostic relevance in AD.

Keywords: Alzheimer's disease; deep cervical lymph nodes; brain–cervical lymphatic axis; germinal centers; postoperative prognosis

Background

AD is the most common cause of dementia and is characterized by progressive cognitive decline, impairment in daily functioning, and the accumulation of Aβ plaques and tau-containing neurofibrillary pathology. Although Aβ and tau aggregation are central pathological hallmarks of AD, increasing evidence suggests that impaired clearance of brain-derived solutes and pathological proteins may also contribute to disease progression[1-3]. This has led to growing interest in the glymphatic system, meningeal lymphatic vessels, and downstream cervical lymphatic drainage pathways as important components of central nervous system homeostasis.

The central nervous system was historically considered to have limited conventional lymphatic drainage. However, the discovery of functional meningeal lymphatic vessels has substantially

changed this view[4-6]. Experimental studies have demonstrated that cerebrospinal fluid, interstitial solutes, immune cells, and macromolecules can drain from the central nervous system through meningeal lymphatic pathways toward the cervical lymphatic system. Among these downstream structures, the DCLNs are considered major receiving lymphoid organs for brain-derived lymphatic drainage[7-9]. In animal models of AD, disruption of meningeal lymphatic drainage has been associated with reduced Aβ clearance, enhanced neuroinflammation, and worsened cognitive impairment, whereas enhancement of lymphatic function can improve clearance and attenuate AD-like phenotypes[10, 11]. These findings suggest that the brain–cervical lymphatic axis may be relevant to AD pathophysiology.

DCLNs may represent a peripheral anatomical site where brain-derived pathological material, lymphatic drainage, and immune responses converge. As downstream lymphoid structures of central nervous system drainage, they may participate in the processing of brain-derived antigens, solutes, and cellular components[12, 13]. However, most current evidence linking meningeal lymphatic dysfunction and cervical lymph node involvement to AD derives from preclinical studies, particularly in mouse models showing that impaired meningeal lymphatic drainage aggravates amyloid pathology, alters neuroimmune responses, and worsens cognitive deficits. By contrast, human studies have largely focused on the anatomical or imaging characterization of meningeal lymphatic pathways, and direct histopathological evidence from brain-draining cervical lymph nodes remains scarce[14, 15]. Whether human DCLNs exhibit structural remodeling, AD-related protein deposition, and clinically relevant alterations in patients with AD therefore remains an important unresolved question.

GCs are specialized lymphoid structures involved in antigen-driven B-cell activation, clonal expansion, somatic hypermutation, and antibody affinity maturation. Although GC number alone cannot fully define lymph node function, changes in GC number and organization may provide histological insight into lymphoid architectural integrity[16-19]. In the context of brain-draining lymph nodes, reduced or disorganized germinal centers may reflect altered lymphoid responses to incoming antigens or solutes from the central nervous system. In addition, stromal fibrosis, vascular remodeling, and changes in lymphatic endothelial markers may indicate broader disruption of the lymph node microenvironment[20-23]. These histopathological features may therefore provide a peripheral tissue-based window into the status of the brain–cervical lymphatic axis in AD.

Several important questions remain unresolved in human AD. First, it is unclear whether DCLNs undergo histopathological remodeling in patients with AlD. Second, whether AD-related proteins such as Aβ and tau are detectable within these downstream brain-draining lymph nodes has not been sufficiently characterized. Third, whether structural features of DCLNs, particularly GC number and fibrosis-related remodeling, are associated with cognitive and functional impairment remains unknown. Finally, whether DCLNs histopathology has potential prognostic relevance for postoperative cognitive and functional outcomes has not been investigated. To address these questions, we examined human DCLNs from patients with AD and cognitively unimpaired controls, focusing on GC-related features, nodal histological remodeling, and their relationships with clinical characteristics. We hypothesized that DCLNs exhibit histopathological remodeling in AD and that preserved GCs architecture is associated with better cognitive status and more favorable postoperative improvement.

Methods

Participants and samples

The study cohort included 66 participants (139 lymph nodes) between April 2024 and February 2025. This cohort comprised 59 participants (132 lymph nodes) who underwent deep cervical lymph node venous anastomosis (DCLNVA) surgery for AD, and 7 participants (7 lymph nodes) who were oral cancer patients with no diagnosis of cognitive impairment. They underwent cervical lymph node dissection, provided that the lymph nodes were harvested only after intraoperative frozen section analysis had confirmed the absence of cancer cell metastasis. All AD patients included in this study met the criteria of the National Institute on Aging-Alzheimer's Association (NIA-AA) for moderate to severe AD [24]. The clinical characteristics of the participants were showed in Table 1. All lymph node samples were obtained from surgical specimens after excluding lymph node metastasis of tumor cells and were utilized for subsequent analyses. Immediately after excision, DCLNs tissue was rinsed in phosphate-buffered saline (PBS), fixed in 4% neutral buffered formalin, and stored at 4°C until paraffin embedding. Specimens were processed using standard histopathological workflows.

Hematoxylin–Eosin Staining

Paraffin blocks were sectioned at 4 μm on a rotary microtome (RM2016, Leica, Germany). Six

consecutive sections were prepared per block, with the optimal section mounted on poly-L-lysine–coated glass slides. The first section underwent H&E staining to verify morphological integrity and to enumerate GC; the remaining sections were reserved for multiplex immunofluorescence. Two experienced pathologists independently reviewed H&E slides. Only samples deemed histologically intact by tissue-specific criteria were included for quantitative analysis. Average cell density and GC numbers were quantified using Fiji/ImageJ (v2.9.0; NIH, Bethesda, MD, USA).

Multiplex Immunofluorescence

Qualified sections were processed for multiplex immunofluorescence using primary antibodies to Aβ (Proteintech, rabbit), tau (Zenbio, rabbit), LYVE-1 (Abcam, rabbit), CD31 (Abcam, rabbit), and α-SMA (Proteintech, mouse). After dewaxing and antigen retrieval in EDTA buffer, slides were washed in PBS, endogenous peroxidase activity was quenched, and sections were blocked before overnight incubation with primary antibodies at 4°C. Following PBS washes, appropriate secondary antibodies were applied, and tyramide signal amplification (TSA) was performed. Primary antibodies were stripped by microwave treatment between rounds to enable sequential labelling. Nuclei were counterstained with DAPI; autofluorescence quenching was applied prior to mounting. Images were acquired on a confocal laser scanning microscope (LSM 800). For each lymph node, three randomly selected high-power fields were analyzed; positive areas and fluorescence intensities were quantified in Fiji/ImageJ (v2.9.0). Tau Protein Mean fluorescence intensity (Tau MFI); Aβ Protein Mean fluorescence intensity (Aβ MFI); α-smooth muscle actin Mean fluorescence intensity (α-SMA MFI); Platelet Endothelial Cell Adhesion Molecule-1 Mean fluorescence intensity (CD31 MFI); Lymphatic Vessel Endothelial Hyaluronan Receptor 1 Mean fluorescence intensity (LYVE-1 MFI).

Clinical Data Acquisition

Preoperative cognitive and functional status were assessed by a neurologist using the Mini-Mental State Examination (MMSE), Clinical Dementia Rating–Sum of Boxes (CDR-SB), and Activities of Daily Living (ADL). Assessments were video-recorded for archival purposes, and scores were entered into a study database for analysis. DCLNVA and cervical lymphadenectomy were performed by senior surgeons from relevant specialties; nodes deemed necessary for removal were collected intraoperatively, immediately placed in fixative, and stored at low temperature prior to processing.

Positron emission tomography–computed tomography (PET-CT) Imaging

All patients completed PET-CT examination two weeks before surgery. Fluorodeoxyglucose positron emission tomography (FDG–PET): FDG–PET was performed at Xiangya Hospital following European Association of Nuclear Medicine guidelines[25] . Participants fasted ≥6 h prior to intravenous administration of 185–250 MBq [^{18}F] FDG with stable blood glucose. Static emission imaging commenced 30–45 min post-injection to promote tracer equilibration and optimize signal-to-noise ratio[26] . A 30-min acquisition was obtained as six 5-min frames; subsequent frames were motion-corrected and merged with the first frame. Distribution volume ratio (DVR; DVR = irreversible binding capacity of the full dynamic dataset + 1) images were computed using the multilinear reference tissue model 2 (MRTM2) in PMOD v3.9 [27, 28]. DVR values were extracted from nine PSP target regions in MNI space, defined using basal ganglia parcellations [28], the Brainnetome atlas[29], the Hammers atlas [30], and cadaveric anatomical data [31], including the hypothalamus, substantia nigra, dorsal midbrain, dentate nucleus, dorsolateral prefrontal cortex, and medial prefrontal cortex. Standardized uptake value ratios (SUVr) were also calculated from target and reference regions over a single frame.

florbetapir 18F positron emission tomography (AV45–PET) and tau positron emission tomography (tau–PET): PET scans were acquired on Siemens PET–CT systems (Hi-Rez Biograph 6; Biograph 6 TruePoint with TrueV; Siemens Healthcare, Erlangen, Germany). Subjects underwent Aβ–PET and tau–PET on the same scanner using head fixation to minimize motion. Low-dose CT preceded each PET for attenuation correction. For Aβ–PET, 150 ± 24 MBq [^{18}F]AV45 (Florbetapir) was administered with a 60-min dynamic acquisition; for tau–PET, 163 ± 10 MBq [^{18}F]AV1451 ([^{18}F]T807) with a 120-min acquisition. Dynamic images were reconstructed by filtered back projection (FBP) into a 128 × 128 matrix with 2-mm isotropic voxels, with correction for attenuation, randoms, scatter, and decay. Image processing and analysis were performed in MIAKAT™ (www.miakat.org). Dynamic PET data were motion-corrected and co-registered; subjects were normalized to MNI space using SPM12, referencing MRI-less methods where appropriate [32, 33]. Original functional and structural images were converted to NIfTI using dcm2niix. Manual origin alignment to the MNI template was performed in SPM12 (Display) to ensure the anterior commissure was within 3 cm of [0, 0, 0] and within 15° of canonical angles. Cerebellar grey matter

(GAAIN mask) served as reference tissue; cerebellar normalization yielded SUVr images from which regional SUVr values were extracted using the AAL atlas. SUVr was defined as

$$\mathrm{SUVR} = \frac{SUV_{Target}}{SUV_{Refrence}}$$

where Target was whole-brain voxels and Reference was the GAAIN cerebellar mask. For AV45, the cortical mean (voi_ctx_2mm.nii; GAAIN) was extracted and Centiloid values computed. FDG–PET SUVr and tau–PET SUVr used CTX01 values as whole-brain averages, while AV45–PET used Centiloid as the whole-brain average.

Statistical Analysis

Analyses were conducted in SPSS v26.0 (IBM, Armonk, NY, USA) and GraphPad Prism v8.0 (GraphPad Software, San Diego, CA, USA). Two-sided $P < 0.05$ was considered statistically significant. Associations were evaluated using Pearson or Spearman correlation as appropriate. Predictors of GC number were analysed using binary logistic regression; determinants of continuous outcomes were assessed using multiple linear regression. Model discrimination was evaluated by receiver operating characteristic (ROC) curves and area under the curve (AUC). Multicollinearity was assessed with variance inflation factors (VIF), and internal validation used 1,000-iteration bootstrap resampling. Decision curve analysis (DCA) quantified net clinical benefit across threshold probabilities. Group differences were tested with independent-samples t-tests or chi-square tests, and are reported as mean ± standard error unless stated otherwise. One-way ANOVA was used for multi-group comparisons, with Brown–Forsythe and Bartlett tests to assess homogeneity of variance.

Results

Differential pathogenic protein expression and fibrosis degree in DCLNs from AD and non-AD patients

Previous studies have reported marked differences in the deposition of pathogenic proteins within DCLNs in AD[34]. In this study, we analyzed differences in age, sex, BMI, disease duration, and years of education between AD patients and non-AD patients using independent-samples t-tests and chi-square tests. No significant differences in clinical characteristics were observed between the two groups (Table 1). Subsequently, we quantitatively compared the expression levels of Aβ and tau

protein in DCLNs between AD and non-AD patients using immunofluorescence staining. The analysis revealed that the expression levels of both proteins were significantly higher in AD DCLNs. Significantly elevated levels of Aβ-positive and tau-positive signals, along with increased α-SMA MFI, are observed in lymph nodes from AD patients compared with non-AD patients (Aβ：2.07% vs. 0.46%; $P < 0.01$; tau: 15.95% vs. 10.36%, $P < 0.05$; α-SMA: 7.73% vs. 3.63%, $p<0.05$). (fig 1a-e) These findings confirm that DCLNs from AD patients exhibit substantially elevated pathogenic protein load and fibrosis degree relative to non-AD individuals.

Table 1 Comparative analysis of clinical characteristics between the AD group and the control group

Analysis of clinical characteristics of the AD group and control group

	AD(*n*=59)	control(*n*=7)	t/X^2	P
Age（year）,Mean±SD [a]	69.22±7.91	66.86±5.18	0.769	0.445
Sex, No.[b]				
male	41	3	1.998	0.158
Female	18	4		
BMI（kg/m^2）,Mean±SD [a]	23.41±4.09	22.58±1.62	1.023	0.32
Disease Duration, No. [b]				
≥5（year）	34	5	0.493	0.483
<5（year）	25	2		
Education, No. [b]				
≥9（year）	31	3	0.235	0.628
<9（year）	28	4		

Table 1 Comparative analysis of clinical characteristics between the AD group and the control group. a, t test; b, chi-square test.

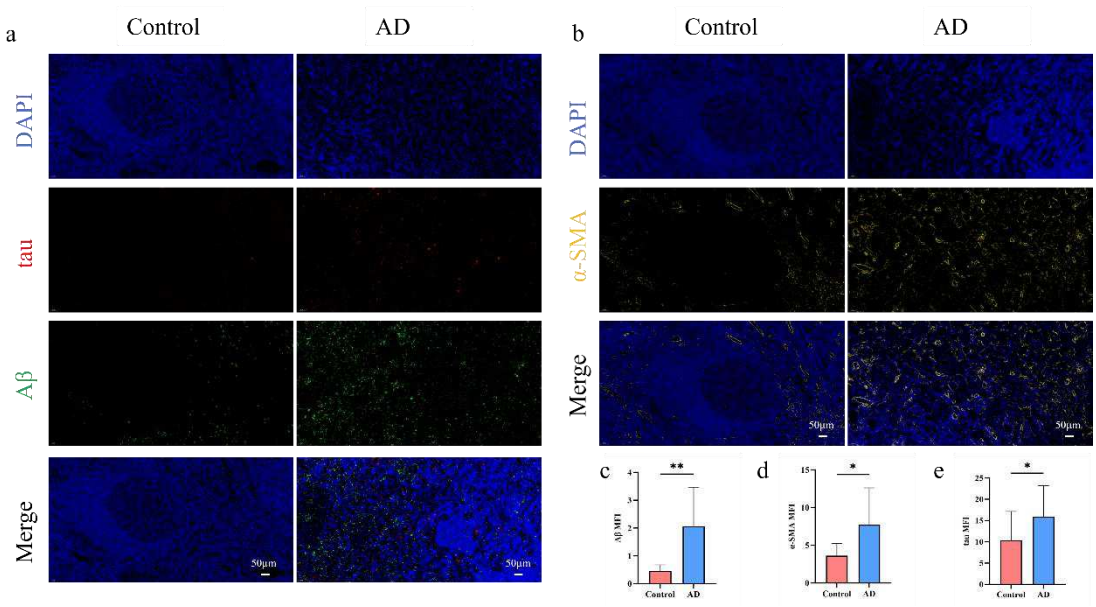


Figure 1　Increased Aβ，tau protein expression and fibrosis degree in DCLNs from AD patients compared with non-AD controls. a.b, Representative immunofluorescence staining of DCLNs from AD and non-AD patients, alongside immunofluorescence images showing Aβ (green) and tau (red) protein expression, scale bar,50 μm, with nuclei counterstained using DAPI (blue). c-e, Quantitative comparison of Aβ, tau, α-SMA mean fluorescence intensity (MFI) between AD and non-AD DCLNs using two-tailed independent-samples t-test. Data are presented as mean ± SEM; statistical significance is indicated as *P < 0.05, **P < 0.01.

Vascular distribution, fibrosis status, and deposition of pathogenic proteins associated with pathological changes in AD in different GC-level DCLNs

Based on the statistical analysis of the collected lymph nodes, the percentile values of GC numbers were as follows: 25th percentile = 0, 50th percentile = 1, and 75th percentile = 4. Considering that 60 lymph nodes had a GC number of 0, we classified the lymph nodes into three levels according to the number of GC: level I (>4 GC), level II (1–4 GC), and level III (no detectable GC). The HE results and corresponding intraoperative immediate lymph node images were showed in Fig.2 a-b. The degree of fibrosis, and the deposition of pathogenic proteins gradually worsen with the increase in lymph node GC level（Fig.2c-e）. Quantitative analysis showed no statistically significant difference in Aβ MFI among levels, although a non-significant upward trend was observed with increasing level. In contrast, tau MFI and α-SMA MFI were significantly elevated in level III compared with level I (*P < 0.05), with intermediate values for level II. Differences between level I

and level II, and between level II and level III, did not reach significance but followed the same increasing trend. Cognitive measures varied with GC level. MMSE, CDR-SB and ADL scores were all significantly different between patients represented by level I versus level III nodes (MMSE, CDR-SB positive correlation; ADL negative correlation in level; *$p < 0.05$, **$p < 0.01$, ****$p < 0.0001$). MMSE was also lower in patients with level II compared with level I nodes, and ADL scores were reduced in level III compared with level II. Overall, higher GC levels were associated with greater tau and α-SMA deposition, and lower cognitive scores, consistent with a structural and molecular profile potentially linked to impaired lymphatic and neuronal function (Fig.2f-k).

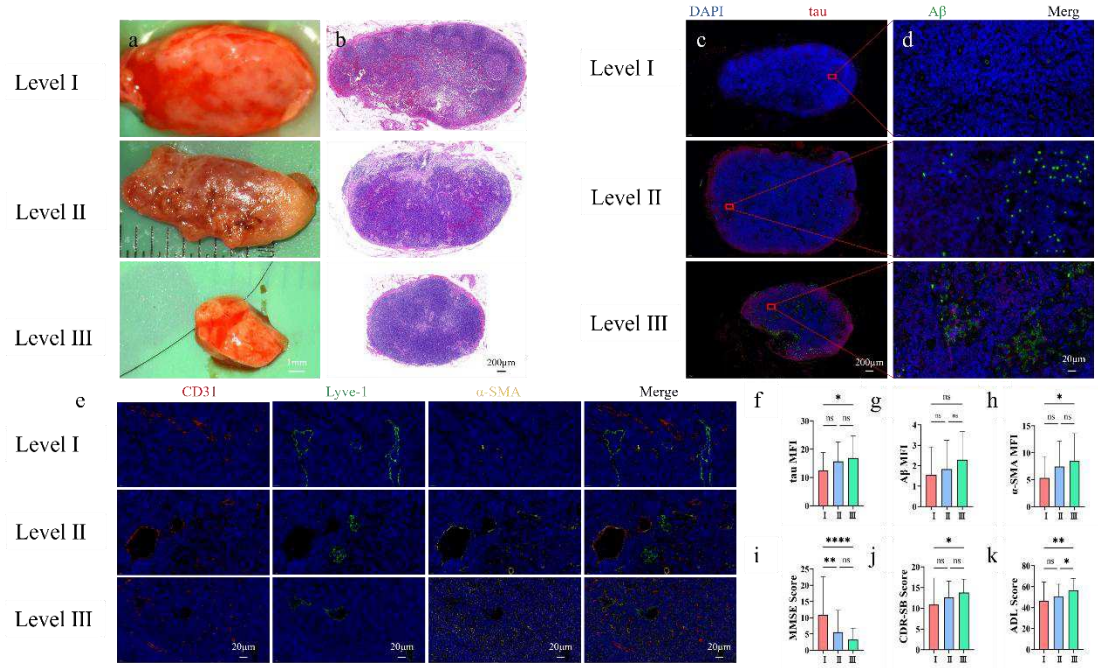


Figure 2 Grading based on the number of GC, patients represented by level I and level III DCLN show significant differences in cognitive function. a-e, DCLNs were classified into three levels according to GC numbers: level I (>4 GC), level II (1–4 GC), and level III (no detectable GC). Representative light microscopy images of lymph nodes at each level, shown at the same magnification(a), scale bar, 1 mm; H&E staining images(b), scale bar, 200 μm. Immunofluorescence staining for Aβ (green) and tau (red) proteins for each level (c), scale bar, 200 μm; with nuclei counterstained using DAPI (blue). Insets show 63× magnification of the same regions (d), scale bar, 20 μm. Immunofluorescence staining of CD31(red), LYVE-1(green), and α-SMA MFI (yellow) for each level lymph nodes (e), scale: 20μm. f-k, Classify different

DCLNs according to the number of GC, and compare the differences in tau MFI (f), A β MFI (g), and α - SMA MFI (h) among each group of lymph nodes through one-way analysis of variance, as well as the differences in MMSE Score (i), CDR-SB Score (j), and ADL Score (k) scores represented by DCLNs among patients. (*p<0.05， ** p<0.01， ****p<0.0001).

Correlation analysis of different indicators with the GC level

Our previous work demonstrated significant differences in MMSE, CDR-SB, and ADL scores, tau and Aβ protein deposition, and lymph node fibrosis across DCLN levels. To further investigate the association between histopathological changes in human DCLNs and the clinical characteristics of patients, we employed Pearson's and Spearman's correlation analyses. The relationships among multiple key variables—including MMSE, CDR-SB, ADL, tau protein deposition, Aβ protein deposition, GC number, cell density, tau MFI, Aβ MFI, α-SMA MFI, LYVE-1 MFI, CD31 MFI, FDG-PET, AV45-PET, and tau-PET—were assessed and visualised in a heatmap. Correlation coefficients ranged from −0.842 to 0.904 (Fig. 3a). Representative scatter plots of selected correlations between DCLN histological staining parameters and patient clinical features were showed in Supplemental Fig. 1.

MNI-SUVr-FDG images depict cerebral glucose metabolism assessed by FDG-PET, normalized to the MNI standard space and expressed as SUVr relative to a reference region. Metabolically active areas are shown in red, with reference areas in blue. The adjacent vertical color bar indicates semi-automated cortical and cerebellar SUVr quantification range; the red maximum corresponds to approximately 2 SUVr units. MNI-SUVr-AV45 images represent β-amyloid deposition quantified by AV45-PET, also normalized to MNI standard space and expressed as SUVr relative to a reference region. Regions of Aβ deposition are shown in red, with reference areas in blue. The vertical color bar indicates cortical and cerebellar SUVr quantification; the red maximum corresponds to approximately 3 SUVr units. Differences in maximal SUVr values between FDG-PET and AV45-PET reflect distinct biological characteristics of cerebral glucose metabolism versus Aβ deposition (Fig.4).

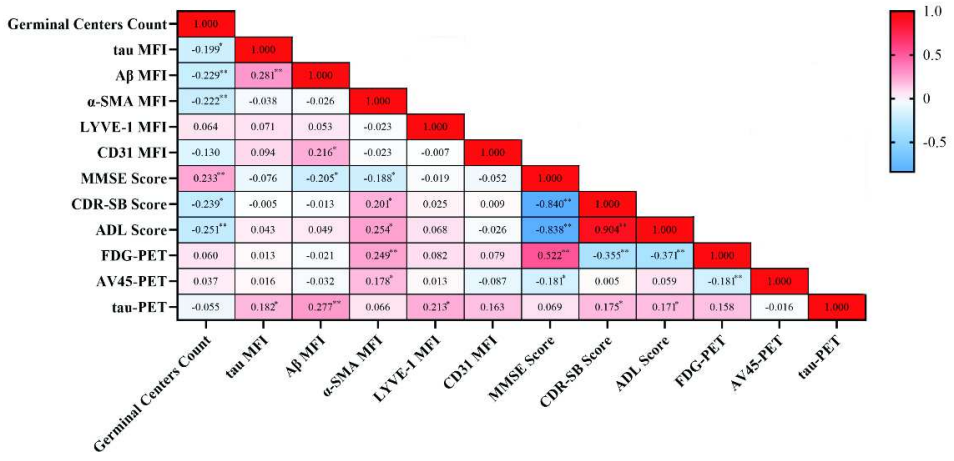


Figure 3 Correlation analysis of GC number with cognitive function, Aβ and tau deposition, and fibrosis in DCLNs. a, Heatmap showing correlation patterns among multiple variables related to DCLN histology and patient clinical parameters. Blue represents negative correlation and red represents positive correlation. Statistical significance is indicated as *P < 0.05, **P < 0.01.

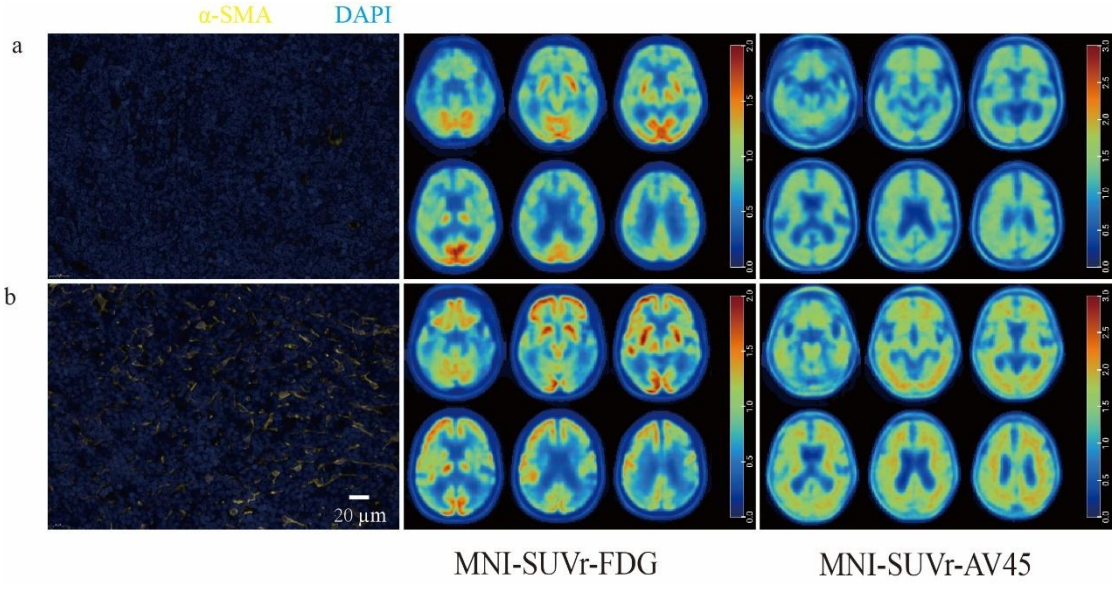


Figure 4 Degree of fibrosis in DCLNs of AD patients is positively associated with brain glucose metabolism and Aβ accumulation. a, Representative immunofluorescence images of DCLNs and corresponding PET-CT scans from a patient with low fibrosis degree. b, Representative images from a patient with high fibrosis degree. The left panels show α-SMA immunofluorescence staining in DCLNs, where nuclei are labeled with DAPI (blue), and α-SMA is indicated in yellow. Scale bar = 20 μm.

Logistic regression analysis and prognostic analysis among DCLNs with different GC numbers

A total of 66 patients and 139 DCLNs were included in the analysis. Based on the number of GCs and the morphology of lymph nodes observed during the operation, lymph nodes were stratified into two groups (GCs ≤4 vs. GCs >4). Baseline demographic and clinical characteristics were compared between the two groups using independent-sample *t* tests or chi-square tests, as appropriate, with detailed data presented in the Supplemental Table 1. When performing statistical analysis, to reduce Type I errors, we used the average value of different lymph node data from the same patient to ensure the correspondence between lymph nodes and patients.

Overall, patients in the GCs ≤4 group showed worse cognitive and functional status than those in the GCs >4 group. Although age and BMI were comparable between the two groups, patients with GCs ≤4 had lower MMSE scores and higher CDR-SB and ADL scores, indicating more severe cognitive impairment and functional decline. In contrast, patients with GCs >4 demonstrated relatively better cognitive performance and daily living ability. The differences in cognitive and functional assessments between the two groups were statistically significant ($P < 0.05$), suggesting that a lower GC number in DCLNs was associated with more severe clinical impairment.

Univariate analysis showed that there were statistically significant differences in tau MFI, α-SMA MFI, MMSE Score, CDR-SB Score, ADL Score. In the multivariate logistic regression analysis, α-SMA MFI and MMSE score were independently associated with the presence of >4 GCs. Specifically, higher α-SMA MFI was associated with a lower likelihood of having >4 GCs (OR = 0.868, 95% CI: 0.760–0.992, $P < 0.05$), whereas a higher MMSE score was associated with an increased likelihood of having >4 GCs (OR = 1.220, 95% CI: 1.048–1.421, $P < 0.05$).

The logistic regression analysis results were showed in Table 2.

To assess the discriminative performance of the logistic regression model incorporating tau MFI, α-SMA MFI, MMSE score, CDR-SB score, and ADL score, ROC curve analysis was performed (Fig. 5a). The AUC for MMSE score was 0.629 (95% CI: 0.479–0.763, $P < 0.05$), with an optimal cutoff value of 8, corresponding to a sensitivity of 87.1% and a specificity of 43.5%. The AUC for α-SMA MFI was 0.681 (95% CI: 0.559–0.793, $P < 0.05$). Variance inflation factor analysis showed no significant multicollinearity among the included variables. In addition, bootstrap resampling with 1,000 iterations demonstrated stable predictive performance ($P < 0.05$), supporting the robustness

of the model. Decision curve analysis further indicated that the model provided a positive net clinical benefit within a threshold probability range of 0.73 to 0.90 (Fig. 5b).

To determine whether this grouping has clinical significance, we conducted follow-up on patients with a GC number of ≤4 and >4. After 6 months of postoperative follow-up, we compared changes in cognitive function before and after surgery. The results showed that patients with GCs >4 exhibited greater postoperative cognitive improvement. Specifically, MMSE scores increased after surgery in both groups, with a more pronounced increase observed in patients with GCs >4（MMSE score change: 0.66 vs. 1.52, P < 0.01; Fig. 6a）. CDR scores decreased more significantly in the GCs >4 group（CDR score change: 0.31 vs. -0.52, P < 0.05; Fig. 6b）. Similarly, ADL scores showed a greater reduction in patients with GCs >4（ADL score change: 0.91 vs. -1.30, P < 0.05; Fig. 6c）. These follow-up data suggest that patients with GCs >4 may achieve better prognostic outcomes after DCLVC surgery.

Table 2 The univariable logistic regression analysis on the number of GCs.

	Single logisitics		Binary logistics（forward）		
	OR (95%CI)	P	Adjusted OR (95%CI)	P	VIF
tau MFI	0.919(0.855 ~ 0.989)	**0.024***	0.922(0.847 ~ 0.005)	0.064	6.560
α-SMA MFI	0.862（0.759 ~ 0.978）	**0.021***	0.868（0.760 ~ 0.992）	**0.038***	1.085
MMSE Score	1.100(1.042 ~ 1.162)	**0.001****	1.220(1.048 ~ 1.421)	**0.011***	5.348
CDR-SB Score	0.891(0.810 ~ 0.980)	**0.017***	1.223(0.917 ~ 1.632)	0.171	1.065
ADL Score	0.961(0.930 ~ 0.994)	**0.019***	1.019(0.939 ~ 1.106)	0.652	1.085

Table 2 The univariable logistic regression analysis on the number of GCs. Note: Font bold: * p<0.05 **p<0.01.

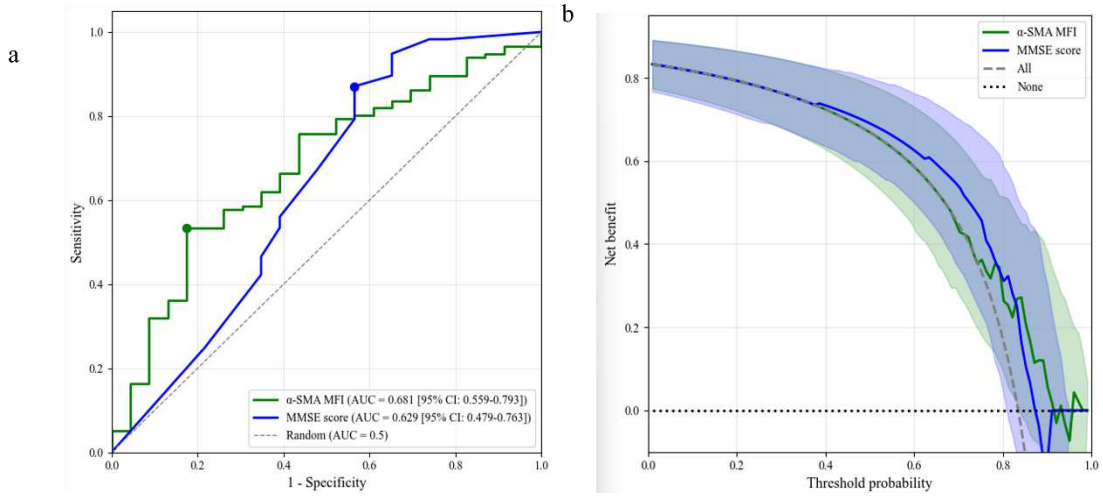


Figure 5 GCs were correlated with both the MMSE score and α-SMA MFI. a, Receiver operating characteristic (ROC) curves for MMSE score (blue) and α-SMA MFI (green), with the diagonal reference line shown in grey. For MMSE score, the AUC was 0.629 (95% CI: 0.479–0.763; $p < 0.05$) with a cut-off value of 8, yielding a specificity of 43.5% and a sensitivity of 87.1%. For α-SMA MFI, the AUC was 0.681 (95% CI: 0.559–0.793; $p < 0.05$) with a cut-off value of 6.65, yielding a specificity of 82.6% and a sensitivity of 53.4%. b, DCA showing the net clinical benefit across different threshold probabilities when using MMSE score or α-SMA MFI to predict GCs >4, Clinical useful threshold range: 0.73 - 0.90, α-SMA MFI, MMSE score: Highly useful. "All" assumes all cases have GCs >4; "None" assumes all cases have GCs ≤4, MMSE score (blue) ; α-SMA MFI (green).

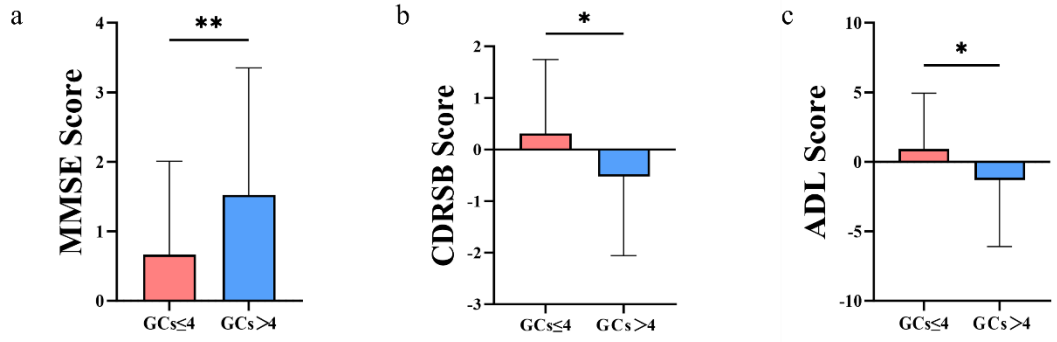
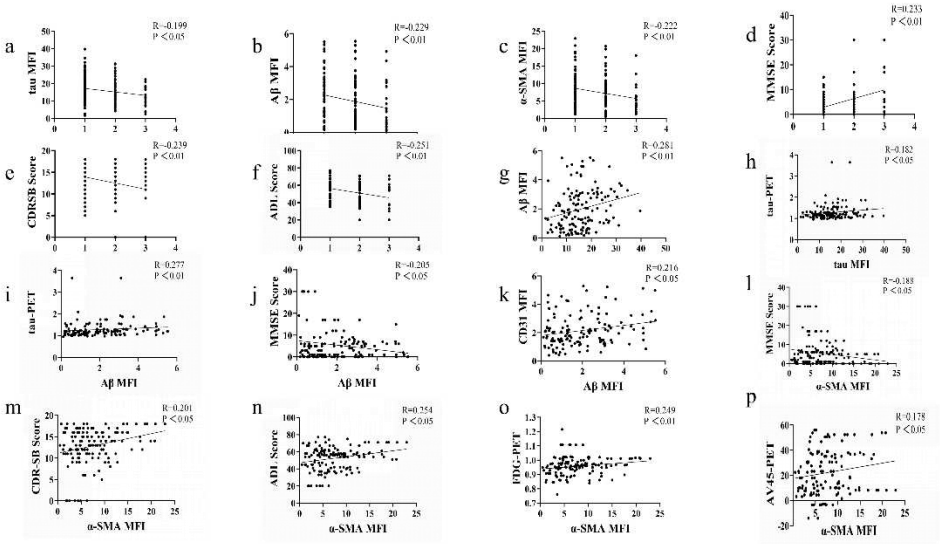


Figure 6 Six-month follow-up data showed that AD patients with more than 4 GCs achieved better cognitive recovery. a-c: Using two-tailed independent-samples t-test, we compared postoperative cognitive outcomes between patients with GCs ≤ 4 and those with GCs > 4, as assessed by DCLN. All data are presented as mean ± SEM, with statistical significance set at *P < 0.05 and **P < 0.01.



Supplemental Figure 1. Representative scatter plots illustrating selected correlations between DCLN histological staining parameters and patient clinical features. Data were analysed using Pearson or Spearman correlation methods, where R denotes the correlation coefficient and P indicates the level of statistical significance. GC number was negatively correlated with tau MFI ($r = -0.190$, $p < 0.05$), Aβ MFI ($\rho = -0.214$, $p < 0.05$), α-SMA MFI ($\rho = -0.245$, $p < 0.01$), CDR-SB score ($r = -0.188$, $p < 0.05$), and ADL score ($\rho = -0.252$, $p < 0.01$), but positively correlated with MMSE score ($\rho = 0.232$, $p < 0.01$). tau MFI in DCLNs exhibited positive correlations with Aβ MFI ($\rho = 0.281$, $p < 0.01$) and tau-PET signal ($\rho = 0.182$, $p < 0.05$). Aβ MFI was negatively correlated with MMSE score ($r = -0.205$, $p < 0.05$), and positively correlated with CD31 MFI ($\rho = 0.216$, $p < 0.05$) and tau-PET ($\rho = 0.277$, $p < 0.01$). Similarly, α-SMA MFI was negatively correlated with MMSE score ($r = -0.188$, $p < 0.05$) and positively correlated with CDR-SB ($\rho = 0.201$, $p < 0.05$), ADL ($\rho = 0.254$, $p < 0.05$), FDG-PET ($\rho = 0.249$, $p < 0.01$), and AV45-PET ($\rho = 0.178$, $p < 0.05$).

Supplemental Table 1 Clinical characteristics of patients represented by different lymph nodes.

	GCs n≤4(*n*=116)	GCs n>4 (*n*=23)	t/X^2	*P*
Age（year）,Mean±SD [a]	70.55±7.28	70.87±6.88	-0.193	0.847
Sex, No.[b]				
male	68	12	0.327	0.568
Female	48	11		
BMI（kg/m^2）,Mean±SD [a]	23.57±4.15	22.78±3.72	0.851	0.396

MMSE Score, Mean±SD [a]	4.39±5.40	10.83±11.75	2.574	**0.017***
CDR-SB Score, Mean±SD [a]	13.27±3.56	10.87±6.41	1.743	0.094
ADL Score, Mean±SD [a]	53.63±11.89	46.30±18.24	1.849	0.076
FDG-PET, Mean±SD [a]	0.96±0.06	0.97±0.07	-0.553	0.331
AV45-PET, Mean±SD [a]	22.77±17.00	18.87±18.72	0.891	0.966
tau-PET, Mean±SD [a]	1.29±0.39	1.24±0.24	0.469	0.691
Disease Duration, No. [b]				
≥5（year）	71	15	0.131	0.718
<5（year）	45	8		
Education, No. [b]				
≥9（year）	64	10	1.054	0.305
<9（year）	52	13		
Comorbidities, No. [b]				
None	90	17	0.548	0.908
Hypertension	14	4		
Diabetes Mellitus	5	1		
Both	7	1		

Supplemental Table 1 Clinical characteristics of patients represented by different lymph nodes. a, t test; b, chi-square test. Statistical significance: * p<0.05; ** p<0.01. P values are from comparisons of lymph node germinal centres adjusted for age, sex, BMI, MMSE score, CDR-SB score, ADL score, PET-CT, disease duration, educational level, and comorbidities. Abbreviations: MMSE, Mini-Mental State Examination; CDR-SB, Clinical Dementia Rating–Sum of Boxes; ADL, Activities of Daily Living; BMI, body mass index; PET-CT, positron emission tomography–computed tomography; FDG-PET, fluorodeoxyglucose positron emission tomography; AV45-PET, florbetapir 18F positron emission tomography; tau-PET, tau positron emission tomography. Mean±SD: mean ± standard deviation.

375

376 **Discussion**

377 In this exploratory human tissue study, we investigated histopathological alterations of DCLNs in
378 patients with AD and examined their associations with cognitive impairment, functional status,

predictive modeling, and 6-month postoperative outcomes. The principal findings were as follows. First, DCLNs from patients with AD showed clear histopathological remodeling, including reduced germinal center number, lymph node structural disruption, fibrosis-related stromal changes, altered vascular and lymphatic marker expression, and detectable Aβ and tau immunoreactivity. Second, patients with lower germinal center GC number, defined as ≤4 (level II-III) GCs, had worse baseline cognitive and functional status than those with >4 (level I) GCs. Third, multivariate logistic regression identified α-SMA mean fluorescence intensity and MMSE score as factors independently associated with preserved GC number. Fourth, receiver operating characteristic and decision curve analyses suggested that the model had predictive performance and potential clinical relevance. Finally, 6-month follow-up showed that patients with >4 GCs had greater postoperative improvement in cognitive and functional measures than patients with ≤4 GCs. Together, these findings suggest that DCLNs histopathology may reflect clinically relevant alterations of the brain–cervical lymphatic axis in AD.

The brain–cervical lymphatic axis has attracted increasing attention in AD research. Glymphatic and meningeal lymphatic pathways contribute to the clearance of cerebrospinal fluid, interstitial solutes, immune cells, and brain-derived macromolecules[35-38]. DCLNs are major downstream lymphoid structures receiving drainage from these pathways. Preclinical studies have shown that impaired meningeal lymphatic drainage can reduce Aβ clearance, enhance neuroinflammation, and worsen cognitive impairment, whereas restoration of lymphatic drainage may improve AD-like phenotypes. However, direct histopathological evidence from human brain-draining lymph nodes remains limited. Our study provides human tissue evidence that DCLNs in AD exhibit structural and molecular alterations, supporting the relevance of downstream lymphoid tissues in AD-related brain drainage and immune communication.

One of the key observations in this study was the reduction of GC number in DCLNs from patients with AD. GCs are specialized lymphoid structures involved in antigen-driven B-cell activation, clonal expansion, somatic hypermutation, and antibody affinity maturation. In aging, GC formation and maintenance may become impaired because of altered B-cell function, defective T-cell help, stromal cell remodeling, chronic inflammatory exposure, and disrupted lymph node architecture[39-44]. Although GC number alone cannot fully define lymph node function, it provides a practical histological indicator of lymphoid architectural integrity. In the context of brain-draining lymph

nodes, reduced germinal center number may reflect altered lymphoid responses to incoming central nervous system-derived antigens, solutes, or cellular components. To provide a descriptive framework for lymph nodes showing different degrees of degenerative remodeling, we further generated an exploratory three-level stratification based on the distribution of GC numbers, using the 25th, 50th, and 75th percentile values as reference points. This approach was intended to capture the histological spectrum of DCLNs remodeling rather than to define a validated functional stage or clinical decision rule. In our cohort, patients with ≤4 germinal centers（level II-III） showed lower MMSE scores and higher CDR-SB and ADL scores, indicating more severe cognitive and functional impairment. This association does not prove that GC loss directly contributes to cognitive decline. Rather, reduced germinal center number may represent a peripheral histological correlate of more advanced AD or impaired brain–cervical lymphatic homeostasis.

The detection of Aβ and tau immunoreactivity in DCLNs further supports the potential involvement of these lymphoid structures in AD-related pathological processes. Aβ and tau are central pathological proteins in AD, and their clearance from the brain may involve multiple pathways, including perivascular, glymphatic, and meningeal lymphatic routes. Because DCLNs are downstream receiving structures of central nervous system drainage, the presence of Aβ and tau signals in these nodes is consistent with the possibility that AD-related proteins, or protein-containing cellular material, may reach peripheral lymphoid tissues. However, the current findings cannot determine the precise origin, biochemical form, or transport route of these proteins. They may represent brain-derived material, locally accumulated proteins, phagocytosed debris, or systemic pathological changes. Future studies using co-localization with macrophage, dendritic cell, B-cell, T-cell, stromal, and lymphatic endothelial markers, together with biochemical validation, will be required to clarify the biological significance of Aβ and tau immunoreactivity in DCLNs.

Fibrosis-related stromal remodeling appeared to be closely linked to germinal center preservation. In the multivariate logistic regression analysis, higher α-SMA mean fluorescence intensity was associated with a reduced likelihood of having >4 GCs. α-smooth muscle actin is commonly used as a marker of activated stromal cells, myofibroblast-like changes, and fibrosis-related remodeling. Increased α-SMA expression within lymph node tissue may indicate stromal activation, extracellular matrix remodeling, and disruption of lymphoid microarchitecture. Such changes may interfere with lymph flow, antigen trafficking, immune cell localization, and maintenance of lymphoid follicles.

Therefore, the inverse association between α-SMA expression and preserved GC number suggests that fibrosis-related remodeling may be an important histological feature of DCLN alteration in AD. In contrast, higher MMSE score was associated with a greater likelihood of preserved GC number. This finding links better cognitive status with relatively preserved lymph node architecture. Several explanations are possible. Preserved GC architecture may reflect better maintenance of lymphoid organization within downstream brain-draining lymph nodes. Alternatively, patients with less severe cognitive impairment may have less pronounced disruption of the brain–cervical lymphatic interface. It is also possible that GC depletion is a downstream marker of more advanced disease burden rather than a causal factor. Because the present study is observational, these possibilities cannot be distinguished. Nevertheless, the association between MMSE score and GCs preservation strengthens the clinical relevance of deep cervical lymph node histopathology in AD.

The ROC and decision curve analyses add an important translational dimension to the study. Rather than only demonstrating group differences, these analyses suggest that combined clinical and histological features may help identify patients with preserved germinal center architecture. ROC analysis supported the discriminative ability of the model, while decision curve analysis suggested potential net clinical benefit across relevant threshold probabilities. These findings are consistent with the concept that DCLNs histopathology may contain clinically meaningful information. However, the predictive model should be regarded as exploratory. It requires external validation in larger, independent cohorts before it can be considered clinically applicable.

The 6-month postoperative follow-up results are particularly important for the clinical interpretation of this study. Patients with >4 GCs showed greater improvement in MMSE, CDR-SB, and ADL scores than patients with ≤4 GCs. This suggests that preserved GC architecture is associated not only with better baseline cognitive and functional status but also with more favorable postoperative recovery. From a translational perspective, this finding raises the possibility that DCLN histopathology may help stratify patients according to postoperative cognitive and functional trajectory. Nevertheless, these results should be interpreted cautiously. Postoperative outcomes may be affected by baseline disease severity, comorbidities, perioperative management, rehabilitation, medication use, and other unmeasured confounders. Therefore, GC number should be considered a potential prognostic correlate rather than a validated predictive biomarker.

Alterations in CD31 and LYVE-1 expression indicate that vascular and lymphatic compartments

may also participate in deep cervical lymph node remodeling in AD. CD31 reflects vascular endothelial structures, whereas LYVE-1 is commonly used as a lymphatic endothelial marker. Changes in these markers may suggest remodeling of blood vascular and lymphatic endothelial niches within the lymph node microenvironment. In brain-draining lymph nodes, such remodeling may influence lymph entry, solute transport, immune cell trafficking, and tissue organization. Together with reduced germinal center number and increased α-SMA expression, these findings suggest that DCLN changes in AD involve multiple structural compartments, including lymphoid follicles, stromal tissue, blood vessels, and lymphatic endothelium.

The present study has several potential implications. Current AD biomarkers mainly include cerebrospinal fluid biomarkers, plasma amyloid and tau measures, neuroimaging, and cognitive assessments. DCLN histopathology is not suitable as a routine diagnostic tool because tissue acquisition is invasive and limited to specific clinical situations. However, our findings provide proof-of-concept evidence that downstream brain-draining lymph nodes may contain histological information related to AD severity and postoperative prognosis. This may broaden the understanding of AD beyond the brain parenchyma alone and highlight the importance of peripheral structures involved in central nervous system drainage and immune communication.

Limitation

Several limitations should be acknowledged. First, this was a single-center exploratory study with a relatively small control group. Because DCLNs cannot be ethically obtained from healthy individuals under ordinary circumstances, control tissues were obtained from cognitively unimpaired surgical patients after excluding metastatic involvement. Potential effects related to surgical indication, tumor background, systemic inflammation, or other clinical factors cannot be completely excluded. Second, most patients with AD in this study had moderate-to-severe disease; therefore, whether similar lymph node alterations occur in prodromal or early-stage AD remains unknown. Third, the study design was observational, and causality between DCLN remodeling, impaired brain drainage, Aβ/tau pathology, and cognitive decline cannot be established. Fourth, GC number is an indirect histological marker and does not fully represent lymph node immune function or lymphatic drainage capacity. Functional lymphatic imaging, immune profiling, and antigen-processing assays were not available. Fifth, Aβ and tau immunoreactivity in lymph nodes requires further validation using additional markers, biochemical assays, and cellular localization studies.

Finally, the logistic regression, ROC analysis, decision curve analysis, and 6-month follow-up results require validation in larger independent cohorts with longer follow-up.

Despite these limitations, this study provides rare human histopathological evidence linking DCLN remodeling with AD severity and postoperative outcome. The integration of tissue morphology, multiplex immunofluorescence, AD-related protein detection, clinical cognitive and functional assessment, predictive modeling, and follow-up data strengthens the translational relevance of the findings. Reduced GC number, increased fibrosis-related remodeling, altered vascular and lymphatic marker expression, and Aβ/tau immunoreactivity together suggest that DCLNs may serve as peripheral histological windows into the brain–cervical lymphatic axis. The association between preserved GC architecture and better baseline cognition as well as greater postoperative improvement further supports the potential prognostic relevance of DCLN histopathology in AD.

Conclusion

In conclusion, this study provides human histopathological evidence that DCLNs are remodeled in AD. These changes include reduced GC number, fibrosis-related stromal remodeling, altered vascular and lymphatic marker expression, and detectable Aβ and tau immunoreactivity. Lower GC number was associated with more severe cognitive and functional impairment, while preserved GC architecture was associated with higher MMSE scores, lower α-SMA expression, and greater improvement in cognitive and functional outcomes at 6-month postoperative follow-up. Although these findings do not establish causality, they suggest that DCLN histopathology may represent a peripheral correlate of brain–cervical lymphatic axis alterations and may have potential prognostic relevance in AD. Larger multicenter studies with independent validation, functional lymphatic assessment, and longer follow-up are needed to confirm these findings and clarify their biological significance.

Ethics Statement

The study was approved by the Institutional Ethics Committee of Central South University (Ethics Approval No. 202405002-2) and informed consent was obtained and certify that the study was performed in accordance with the ethical standards as laid down in the 1964 Declaration of Helsinki and its later amendments or comparable ethical standards. All research articles using human subjects, or datasets from human subjects should discuss how the study addresses the heterogeneity of the disease and at-risk populations.

Author Contributions

G.C. and H.H. contributed equally to this work. J.T., P.W., and L.Q. conceived and supervised the study. G.C. and H.H. designed and performed the experiments, collected samples and clinical data, analyzed the data, prepared the figures, and drafted the manuscript. J.M. and Y.Z. contributed to participant recruitment, neurological evaluation, cognitive and functional assessments, and clinical data interpretation. G.C., H.H., and J.M. performed histological evaluation, multiplex immunofluorescence analysis, and image quantification. L.Q. and P.W. contributed to experimental supervision, pathological assessment, statistical analysis, and interpretation of the results. J.T. provided clinical resources, coordinated the study, supervised the project, and critically revised the manuscript. All authors discussed the results, revised the manuscript, approved the final version, and agree to be accountable for the integrity and accuracy of the work.

Acknowledgements

We would like to express our gratitude to the patients and their families, whose help and participation made this work possible, for their significant contribution to the research on the treatment of Alzheimer's disease. An unauthorized version of the Chinese MMSE was used by the study team without permission, however this has now been rectified with PAR. The MMSE is a copyrighted instrument and may not be used or reproduced in whole or in part, in any form or language, or by any means without written permission of PAR (www.parinc.com).

Data availability

The datasets used or analysed during the current study available from the corresponding author on reasonable request.

Funding

This work was supported by the National Natural Science Foundation of China (Grant No. 82272508), (Grant No. 82572774) and the Natural Science Foundation of Hunan Province (Grant No. 2023JJ30935).

Conflict of Interest statement

The authors declare that they have no competing interests.

References

1. Reeves BC, Karimy JK, Kundishora AJ, Mestre H, Cerci HM, Matouk C, Alper SL, Lundgaard I, Nedergaard M, Kahle KT: **Glymphatic System Impairment in Alzheimer's Disease and**

Idiopathic Normal Pressure Hydrocephalus. *Trends Mol Med* 2020, **26**(3):285-295.

2. Al-Kuraishy HM, Sulaiman GM, Mohammed HA, Al-Gareeb AI, Albuhadily AK, Ali AA, Abu-Alghayth MH: **Beyond amyloid plaque, targeting α-synuclein in Alzheimer disease: The battle continues**. *Ageing Res Rev* 2025, **105**:102684.
3. Becerra-Calixto A, Banerjee A, Fan H, Tan C, Lee E, McCullough LD, Lee J: **A neuroimmune cerebral assembloid model to study the pathophysiology of familial Alzheimer's disease**. *J Neuroinflammation* 2025, **22**(1):227.
4. Da Mesquita S, Papadopoulos Z, Dykstra T, Brase L, Farias FG, Wall M, Jiang H, Kodira CD, de Lima KA, Herz J *et al*: **Meningeal lymphatics affect microglia responses and anti-Aβ immunotherapy**. *Nature* 2021, **593**(7858):255-260.
5. Louveau A, Smirnov I, Keyes TJ, Eccles JD, Rouhani SJ, Peske JD, Derecki NC, Castle D, Mandell JW, Lee KS *et al*: **Structural and functional features of central nervous system lymphatic vessels**. *Nature* 2015, **523**(7560):337-341.
6. Louveau A, Plog BA, Antila S, Alitalo K, Nedergaard M, Kipnis J: **Understanding the functions and relationships of the glymphatic system and meningeal lymphatics**. *J Clin Invest* 2017, **127**(9):3210-3219.
7. Proulx ST: **Cerebrospinal fluid outflow: a review of the historical and contemporary evidence for arachnoid villi, perineural routes, and dural lymphatics**. *Cell Mol Life Sci* 2021, **78**(6):2429-2457.
8. McDonald DM, Alitalo K, Betsholtz C, Engelhardt B, Proulx ST, Siegenthaler J, Koh GY: **Cerebrospinal fluid draining lymphatics in health and disease: advances and controversies**. *Nat Cardiovasc Res* 2025, **4**(9):1047-1065.
9. Ringstad G, Eide PK: **Molecular trans-dural efflux to skull bone marrow in humans with CSF disorders**. *Brain* 2022, **145**(4):1464-1472.
10. Da Mesquita S, Fu Z, Kipnis J: **The Meningeal Lymphatic System: A New Player in Neurophysiology**. *Neuron* 2018, **100**(2):375-388.
11. Da Mesquita S, Louveau A, Vaccari A, Smirnov I, Cornelison RC, Kingsmore KM, Contarino C, Onengut-Gumuscu S, Farber E, Raper D *et al*: **Functional aspects of meningeal lymphatics in ageing and Alzheimer's disease**. *Nature* 2018, **560**(7717):185-191.
12. Gursky Z, Khan ZN, Koundal S, Bhardwaj A, Caceres Melgarejo J, Xu K, Chen X, Lin HM, Gu X, Lee H *et al*: **Age-dependent brain responses to mechanical stress determine resilience in a chronic lymphatic drainage impairment model**. *J Clin Invest* 2025, **135**(17).
13. Zhao MY, Ye CY, Liu YC, Wang XM, Fu JC, Liu XY, Zhu R, Li YZ, Tian Q: **Role of meningeal lymphatic vessels in brain homeostasis**. *Front Immunol* 2025, **16**:1593630.
14. Albayram MS, Smith G, Tufan F, Tuna IS, Bostancıklıoğlu M, Zile M, Albayram O: **Non-invasive MR imaging of human brain lymphatic networks with connections to cervical lymph nodes**. *Nat Commun* 2022, **13**(1):203.
15. Shan X, Lu Y, Luo Z, Zhao X, Pang M, Yin H, Guo X, Zhou H, Zhang J, Huang J *et al*: **A Long-Acting Lyotropic Liquid Crystalline Implant Promotes the Drainage of Macromolecules by Brain-Related Lymphatic System in Treating Aged Alzheimer's Disease**. *ACS Nano* 2024, **18**(13):9688-9703.
16. Silva-Cayetano A, Linterman MA: **Stromal cell control of conventional and ectopic germinal centre reactions**. *Curr Opin Immunol* 2020, **64**:26-33.

17. Kim W, Zhou JQ, Horvath SC, Schmitz AJ, Sturtz AJ, Lei T, Liu Z, Kalaidina E, Thapa M, Alsoussi WB *et al*: **Germinal centre-driven maturation of B cell response to mRNA vaccination**. *Nature* 2022, **604**(7904):141-145.
18. Dempsey LA: **Aging lymph node responses**. *Nat Immunol* 2022, **23**(6):817.
19. Luscieti P, Hubschmid T, Cottier H, Hess MW, Sobin LH: **Human lymph node morphology as a function of age and site**. *J Clin Pathol* 1980, **33**(5):454-461.
20. Sarkkinen J, Yohannes DA, Kreivi N, Dürnsteiner P, Elsakova A, Huuhtanen J, Nowlan K, Kurdo G, Linden R, Saarela M *et al*: **Altered immune landscape of cervical lymph nodes reveals Epstein-Barr virus signature in multiple sclerosis**. *Sci Immunol* 2025, **10**(104):eadl3604.
21. Damato V, Theorell J, Al-Diwani A, Kienzler AK, Makuch M, Sun B, Handel A, Akdeniz D, Berretta A, Ramanathan S *et al*: **Rituximab abrogates aquaporin-4-specific germinal center activity in patients with neuromyelitis optica spectrum disorders**. *Proc Natl Acad Sci U S A* 2022, **119**(24):e2121804119.
22. Angeli V, Ginhoux F, Llodrà J, Quemeneur L, Frenette PS, Skobe M, Jessberger R, Merad M, Randolph GJ: **B cell-driven lymphangiogenesis in inflamed lymph nodes enhances dendritic cell mobilization**. *Immunity* 2006, **24**(2):203-215.
23. Chyou S, Ekland EH, Carpenter AC, Tzeng TC, Tian S, Michaud M, Madri JA, Lu TT: **Fibroblast-type reticular stromal cells regulate the lymph node vasculature**. *J Immunol* 2008, **181**(6):3887-3896.
24. Jack CR, Jr., Andrews JS, Beach TG, Buracchio T, Dunn B, Graf A, Hansson O, Ho C, Jagust W, McDade E *et al*: **Revised criteria for diagnosis and staging of Alzheimer's disease: Alzheimer's Association Workgroup**. *Alzheimers Dement* 2024, **20**(8):5143-5169.
25. Guedj E, Varrone A, Boellaard R, Albert NL, Barthel H, van Berckel B, Brendel M, Cecchin D, Ekmekcioglu O, Garibotto V *et al*: **EANM procedure guidelines for brain PET imaging using [(18)F]FDG, version 3**. *Eur J Nucl Med Mol Imaging* 2022, **49**(2):632-651.
26. Signorini M, Paulesu E, Friston K, Perani D, Colleluori A, Lucignani G, Grassi F, Bettinardi V, Frackowiak RS, Fazio F: **Rapid assessment of regional cerebral metabolic abnormalities in single subjects with quantitative and nonquantitative [18F]FDG PET: A clinical validation of statistical parametric mapping**. *Neuroimage* 1999, **9**(1):63-80.
27. Ichise M, Liow JS, Lu JQ, Takano A, Model K, Toyama H, Suhara T, Suzuki K, Innis RB, Carson RE: **Linearized reference tissue parametric imaging methods: application to [11C]DASB positron emission tomography studies of the serotonin transporter in human brain**. *J Cereb Blood Flow Metab* 2003, **23**(9):1096-1112.
28. Keuken MC, Bazin PL, Backhouse K, Beekhuizen S, Himmer L, Kandola A, Lafeber JJ, Prochazkova L, Trutti A, Schäfer A *et al*: **Effects of aging on T_1, T_2*, and QSM MRI values in the subcortex**. *Brain Struct Funct* 2017, **222**(6):2487-2505.
29. Fan L, Li H, Zhuo J, Zhang Y, Wang J, Chen L, Yang Z, Chu C, Xie S, Laird AR *et al*: **The Human Brainnetome Atlas: A New Brain Atlas Based on Connectional Architecture**. *Cereb Cortex* 2016, **26**(8):3508-3526.
30. Hammers A, Allom R, Koepp MJ, Free SL, Myers R, Lemieux L, Mitchell TN, Brooks DJ, Duncan JS: **Three-dimensional maximum probability atlas of the human brain, with particular reference to the temporal lobe**. *Hum Brain Mapp* 2003, **19**(4):224-247.
31. Williams DR, Holton JL, Strand C, Pittman A, de Silva R, Lees AJ, Revesz T: **Pathological**

tau burden and distribution distinguishes progressive supranuclear palsy-parkinsonism from Richardson's syndrome. *Brain* 2007, **130**(Pt 6):1566-1576.

32. Doré V, Bullich S, Rowe CC, Bourgeat P, Konate S, Sabri O, Stephens AW, Barthel H, Fripp J, Masters CL *et al*: **Comparison of (18)F-florbetaben quantification results using the standard Centiloid, MR-based, and MR-less CapAIBL(®) approaches: Validation against histopathology**. *Alzheimers Dement* 2019, **15**(6):807-816.
33. Landau SM, Ward TJ, Murphy A, Iaccarino L, Harrison TM, La Joie R, Baker S, Koeppe RA, Jagust WJ: **Quantification of amyloid beta and tau PET without a structural MRI**. *Alzheimers Dement* 2023, **19**(2):444-455.
34. Al-Diwani A, Provine NM, Murchison A, Laban R, Swann OJ, Koychev I, Sheerin F, Da Mesquita S, Heslegrave A, Zetterberg H *et al*: **Neurodegenerative fluid biomarkers are enriched in human cervical lymph nodes**. *Brain* 2025, **148**(2):394-400.
35. Lahmar T, Thuau F, Pinard G, Boutoleau-Bretonniere C, Perrot P, Lancien U: **Brain lymphatic drainage pathways, deep cervical lymphatic surgery, and current insights: A systematic review**. *J Prev Alzheimers Dis* 2026, **13**(1):100335.
36. Feng Y, Wang S, Xia H, Jiang X, Wu M, Pan S, Song W: **Meningeal lymphatics as a therapeutic target for neurodegenerative disorders**. *Transl Neurodegener* 2025, **14**(1):65.
37. Hitpass Romero K, Stevenson TJ, Smyth LCD, Watkin B, McCullough SJC, Vinnell L, Smith AM, Schweder P, Correia JA, Kipnis J *et al*: **Age-related meningeal extracellular matrix remodeling compromises CNS lymphatic function**. *J Neuroinflammation* 2025, **22**(1):109.
38. Rojas Velazquez MN, Gousopoulos E, Wolf S, Zurfluh CE, Lindenblatt N: **Ageing and the lymphatic system: Implications for immunity, brain health, and possible therapeutic interventions**. *Ageing Res Rev* 2026, **118**:103126.
39. Denton AE, Dooley J, Cinti I, Silva-Cayetano A, Fra-Bido S, Innocentin S, Hill DL, Carr EJ, McKenzie ANJ, Liston A *et al*: **Targeting TLR4 during vaccination boosts MAdCAM-1(+) lymphoid stromal cell activation and promotes the aged germinal center response**. *Sci Immunol* 2022, **7**(71):eabk0018.
40. Zheng B, Han S, Takahashi Y, Kelsoe G: **Immunosenescence and germinal center reaction**. *Immunol Rev* 1997, **160**:63-77.
41. Masters AR, Hall A, Bartley JM, Keilich SR, Lorenzo EC, Jellison ER, Puddington L, Haynes L: **Assessment of Lymph Node Stromal Cells as an Underlying Factor in Age-Related Immune Impairment**. *J Gerontol A Biol Sci Med Sci* 2019, **74**(11):1734-1743.
42. Denton A, Silva-Cayetano A, Dooley J, Hill D, Carr E, Robert P, Meyer-Hermann M, Liston A, Linterman M: **Intrinsic defects in lymph node stromal cells underpin poor germinal center responses during aging**. *bioRxiv* 2020.
43. Aydar Y, Balogh P, Tew JG, Szakal AK: **Age-related depression of FDC accessory functions and CD21 ligand-mediated repair of co-stimulation**. *Eur J Immunol* 2002, **32**(10):2817-2826.
44. Lefebvre JS, Masters AR, Hopkins JW, Haynes L: **Age-related impairment of humoral response to influenza is associated with changes in antigen specific T follicular helper cell responses**. *Sci Rep* 2016, **6**:25051.

Supplementary Files

This is a list of supplementary files associated with this preprint. Click to download.

- SupplementalFigureLegend.docx
- SupplementalTable1.docx